JOINT INSTITUTE FOR NUCLEAR RESEARCH
Laboratory of Nuclear Problems named after Djelepov

FINAL REPORT ON THE START PROGRAMME

Investigating of some physical properties of scintillator strips and fluoroplastic membranes

Supervisor:
Artikov A.M.
Chokheli D.S.

Student:
Inoyatillo Ozoda, Samarkand State University

Participation period:
September 01 – October 12, Summer Session 2024

Dubna, 2024

Contents:

Abstract

Detectors based on a plastic scintillator are widely used in most modern experiments in High Energy Physics. Typically, the sufficient detection efficiency of such systems for minimum ionizing particles is more than 90%. However, some experiments should use a so-called active shield system against background muons, particularly cosmic muons: cosmic muons should first be detected and rejected through online/offline data processing. We call such a system a Cosmic Ray Vita (CRV) system. The CRV system always requires a higher muon detection efficiency than regular muon systems. For instance, both the Mu2e experiment [1] (FNAL, USA) and the COMET experiment [2] (KEK, Japan) require the CRV system detection efficiency to be equal to or better than 99.99% to establish sufficient suppression of the cosmic background and thus achieve the required sensitivity of these experiments in the order of 10-17 for a so-called single-event -- for a direct conversion of the muon into the electron.

I. Introduction

The Standard Model (SM) not only effectively describes the properties of elementary particles and their interactions as observed in experiments, but it also possesses strong predictive power. However, despite its successes, the SM does not provide explanations for several phenomena, such as the presence or absence of dark matter, the observed asymmetry between matter and antimatter, and neutrino oscillations, among others. These processes are being explored through Beyond Standard Model (BSM) physics, which seeks to understand phenomena beyond the framework of the SM.
One intriguing process is the direct (neutrino-less) transition of a muon into an electron, which would indicate a violation of lepton number conservation (Charged Lepton Flavor Violation, CLFV). This falls within the realm of BSM physics. Currently, several experiments are planned to potentially detect CLFV processes, such as the Mu2e experiment at Fermilab (Batavia, USA) and the COMET experiment at KEK/J-PARC (Japan).

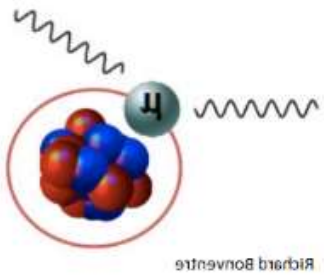

Fig.1 Muon conversion into electron

1.1 Main Objective

The main aim of this project is to acquire basic knowledge of the C++ programming language and the ROOT software framework and to utilize them for data processing. Additionally, the primary physical objectives were: first to find the optimal exposure time of etching for creating the scintillator reflection surface by conducting experiments with cosmic rays; and second, to study the wrapping material made of fluoroplastic.

1.2 Foundation of ROOT

ROOT is a software framework for data analysis and Input/Output: a powerful tool to cope with the demanding tasks typical of state of the art scientific data analysis. It provides all the functionality needed for big data processing, statistical analysis, visualization and storage. Among its prominent features is an advanced graphical user interface, ideal for interactive analysis, an interpreter for the C++ programming language, for rapid and efficient prototyping and a persistency mechanism for C++ objects, used also to write every year petabytes of data recorded by the Large Hadron

Collider experiments. This introductory guide illustrates the main features of ROOT which are relevant for the typical problems of data analysis: input and plotting of data from measurements and fitting of analytical functions. Daily, thousands of physicists use ROOT applications to analyze their data or for modeling.

II. COMET(COherent Muon to Electron Transition)

The COMET experiment is divided into two phases. In Phase I, the focus is on the construction of up to the first 90° bend and the placement of the detector. Direct beam measurements will be performed; however, there is currently no backward σπ data or real background (BG) data available. The aim is to conduct a μ-e search with intermediate sensitivity, on the order of O(10^-15). Moving on to COMET Phase II, the goal is to complete all transport systems and enhance the μ-e search sensitivity further.

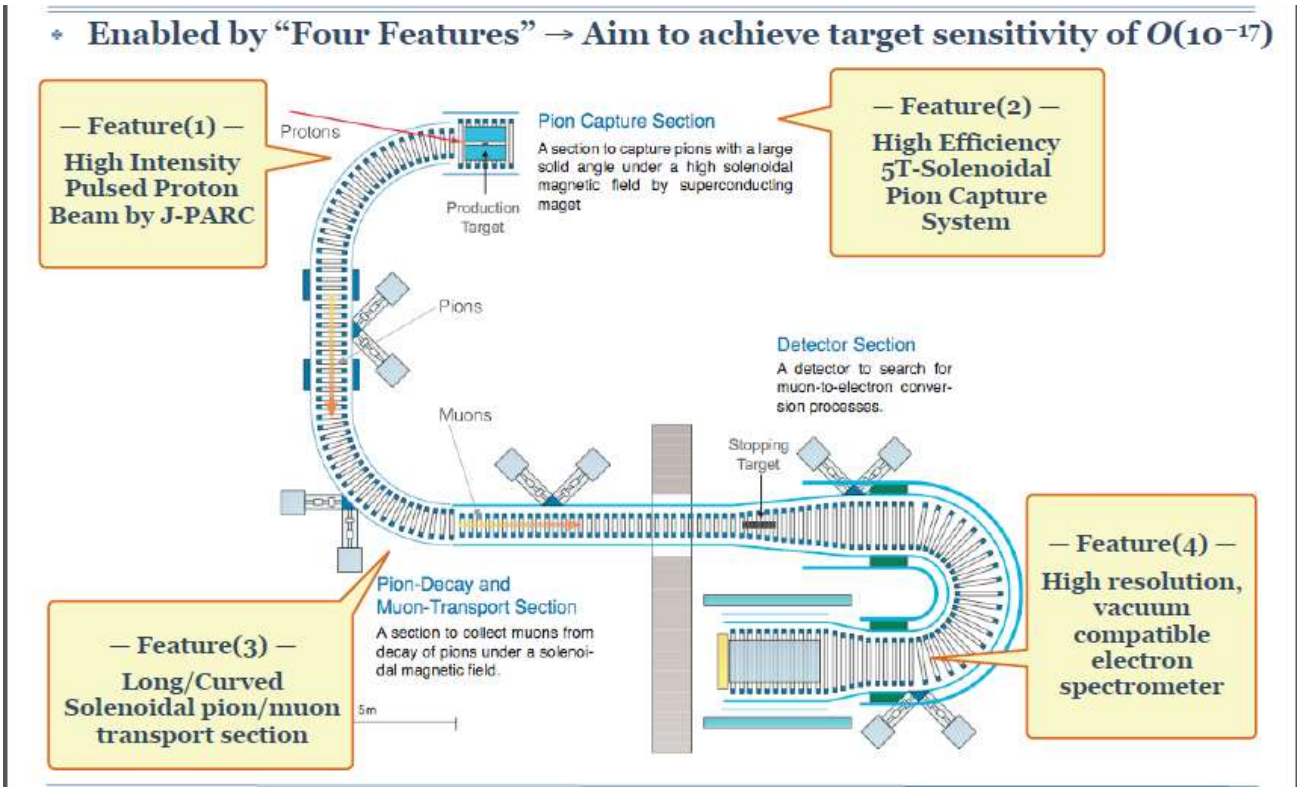

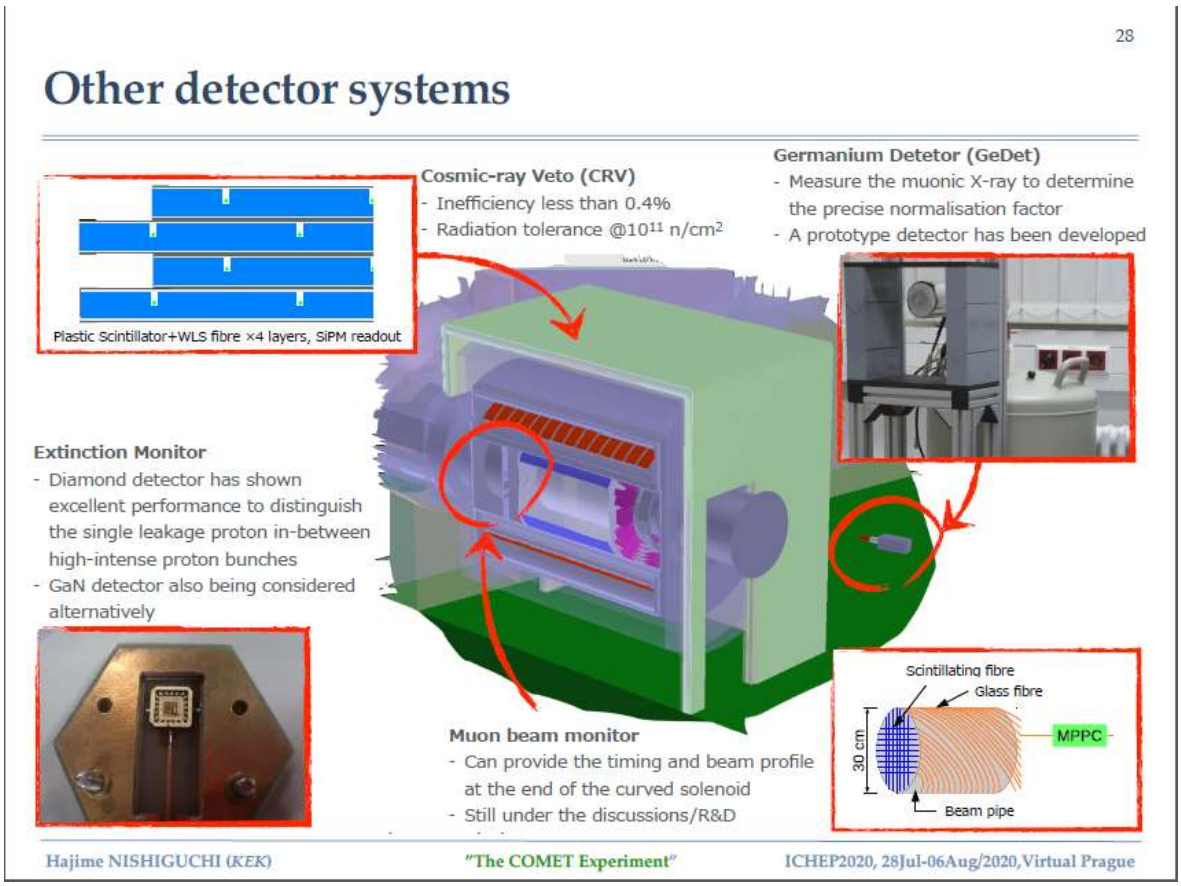

2.1 CRV System

The CRV system itself consists of two main parts: scintillator counter-based (SCRV) and GRP chambers-based (BS-CRV) subsystems. The SCRV subsystem will be located on top of the COMET, on the sides and on the back. Consists of extruded plastic scintillator strips and thin aluminum plates sandwiched between layers of scintillator strips. To carry light, WLS fibers are placed in grooves along the length of the strips. BS-CRV, on the other hand, will be located in COMET's most radiation-laden area, in front of COMET, and will consist of a GRP camera system.

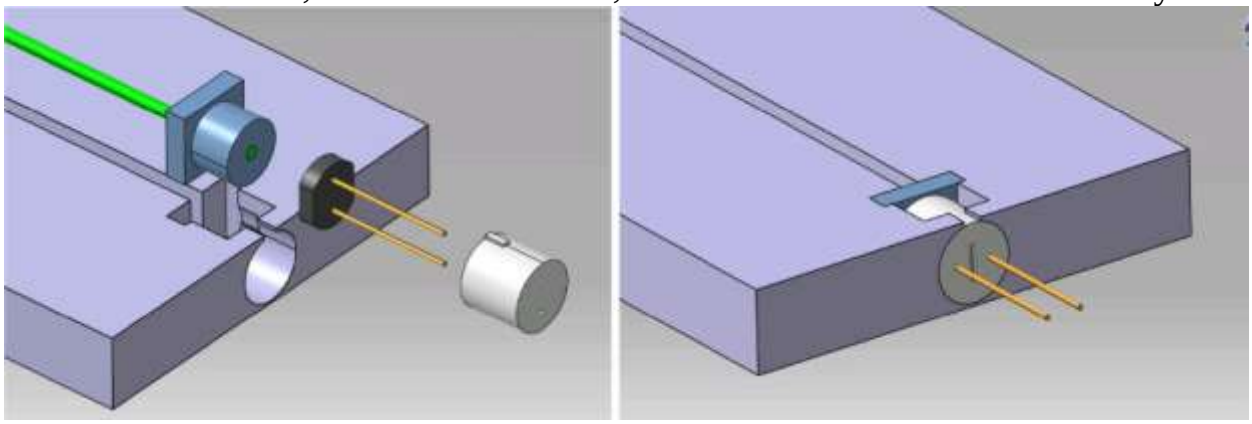

Fig.3 Preliminary design of the CRV system

2.2 Registration of cosmic rays

The scintillation setup consisted of a pair of scintillation strips (7 × 50 × 1000 mm³), with one end of the strips securely attached to the photomultiplier tube (PMT, EM19814). These strips were installed between two trigger units (SiMP Trigger Amp, with plastic scintillator of 40 × 40 × 10 mm³), specifically designed to count cosmic rays. These trigger units had an internal high voltage generator to supply SiPM. The distance between the triggers and the PMT was 400 mm. This arrangement allowed for effective detection and measurement of cosmic radiation within the specified configuration. The voltage on the PMT was set to 1900 volts. Initially, 3000 events were recorded for the pedestal, followed by 3000 events for cosmic rays using the triggers. To collect data for the strips with a particular etching exposure time (of which there were 6 types: 45 minutes, 60 minutes, 90 minutes, 120 minutes, 135 minutes, and 180 minutes), we needed approximately a day. The oscilloscope (HD04104A) could have ability to save data to internal storage and then we could transfer it to PC by USB pen-drive.

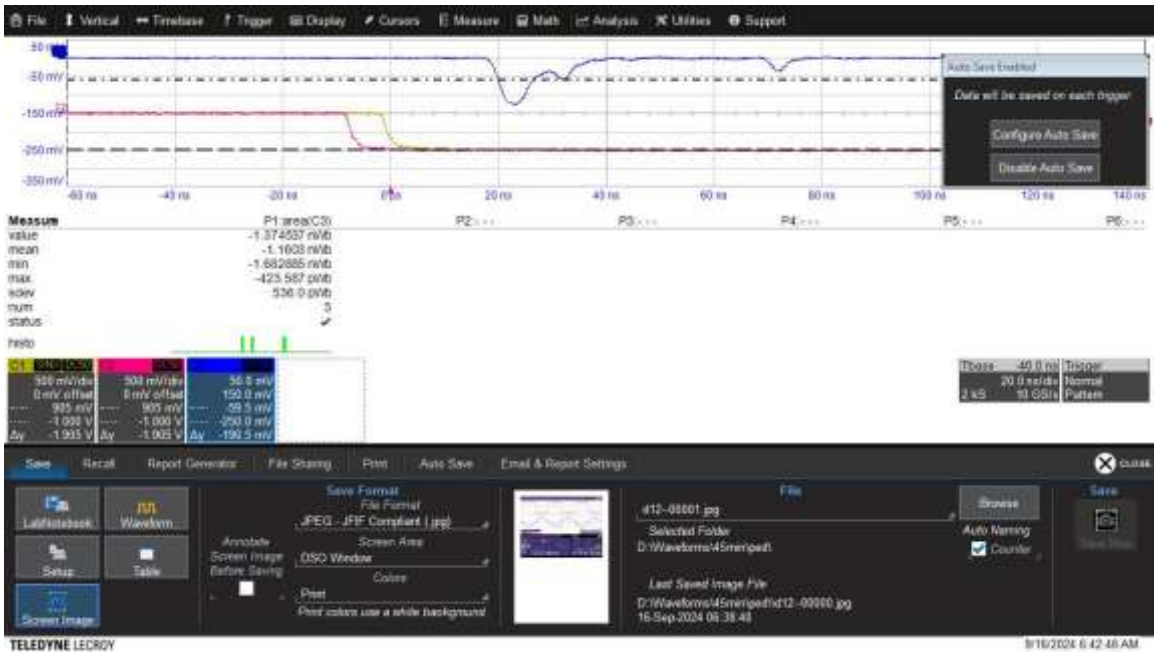

Fig.4 Screen of the oscilloscope
Blue-PMT, red and yellow-triggers.

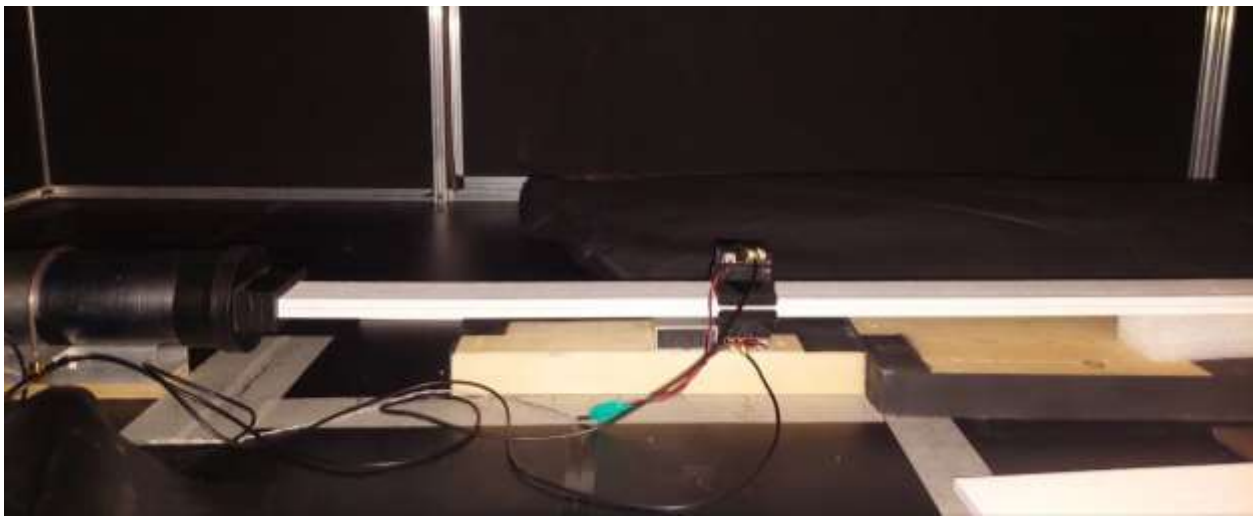

Fig. 5 Experimental equipment

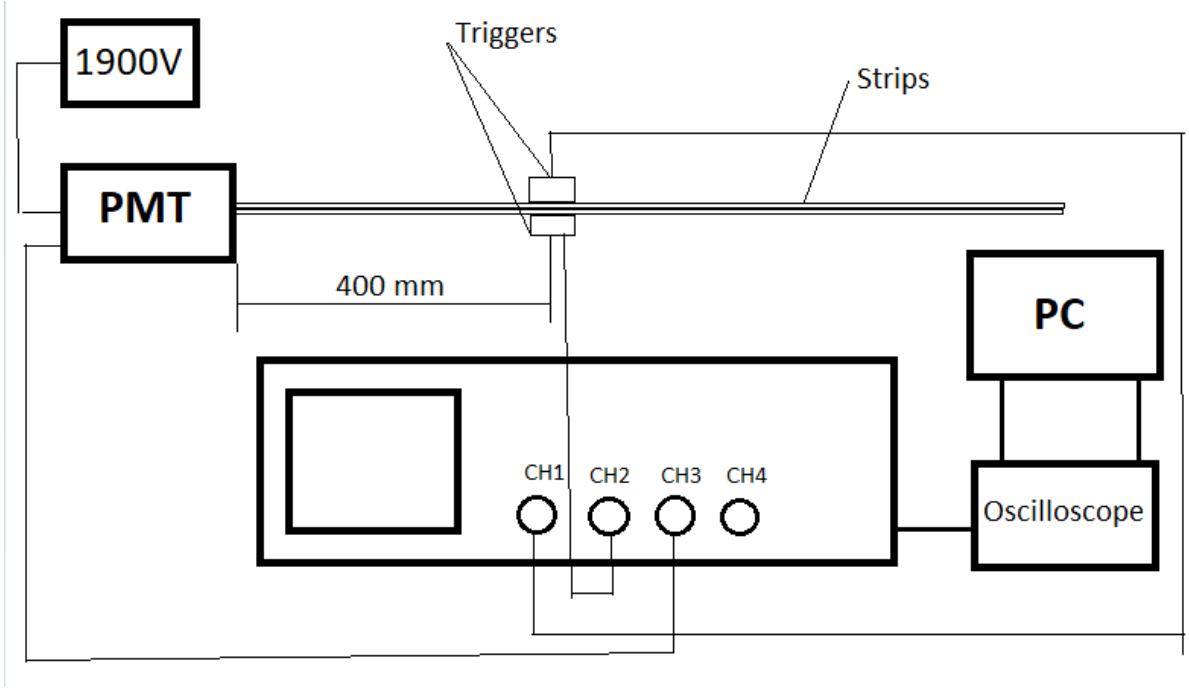

Fig.6 Principal scheme

For the analysis of the collected data, the software based on CERN ROOT with C++ was used. A code was written to subtract the pedestal values from the total recorded values, leaving only the charge values of cosmic particles. Histograms were then created for each exposure time (see Fig. 8). Finally, using TGraphErrors, the dependency of the average charge on the exposure time of the scintillator surfaces was plotted (see Fig. 9). In Fig. 9a, a linear function was fitted, while in Fig. 9b, a parabolic function was used for the fitting.

Although the charge value does not greatly depend on the exposure time, fitting the with parabolic function clearly shows that the optimum could be between 60 and 120 minutes. When the etching exposition time is less than 60 minutes, the thickness

is too small to retain light, and when more than 120 minutes, although the coating thickness is sufficient, the thickness of the scintillator is coming correspondingly smaller, since the coating is obtained by etching the scintillator body with chemicals thus decreasing the scintillation volume and, consequently, light collection deteriorates.

The way how the collected charge calculated

$$q = I*t$$

$$dq = I*dt$$

$$I = U/R=, R=50\Omega$$

$$dq = U/R*t$$

$$dt=0.1ns=10^{(-10)}s$$

$$dq=U*0.02*10^{(-10)}=2*U*10^{(-15)}$$

$$q=2000*2*U*10^{(-15)}=4*U[pC]$$

Calculation of average error

$$б=\sqrt{\frac{StdDev^2}{3000}+\left(\frac{x-x0}{Nbin}\right)^2}$$

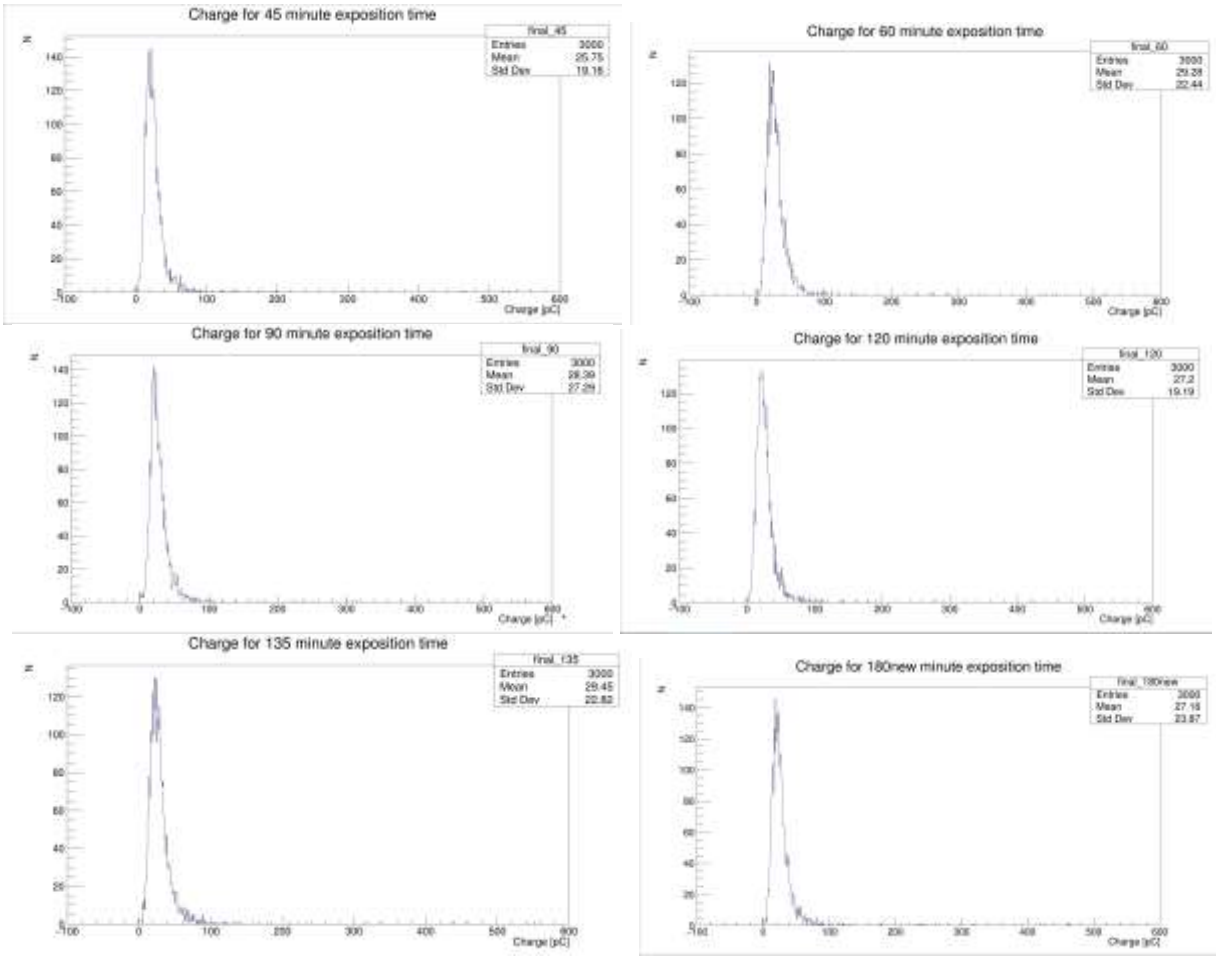

Fig.8 Cosmic data: distribution of the collected charge for different etching exposure times

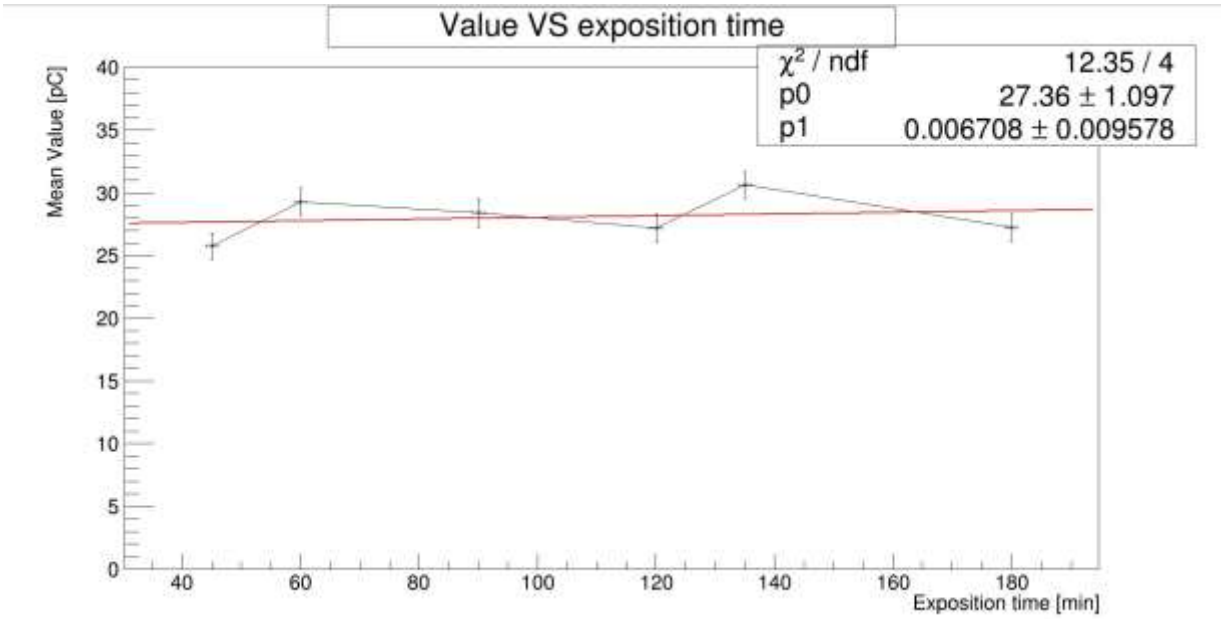

Fig. 9.a Charge value as a function of exposure time fitted by linear function

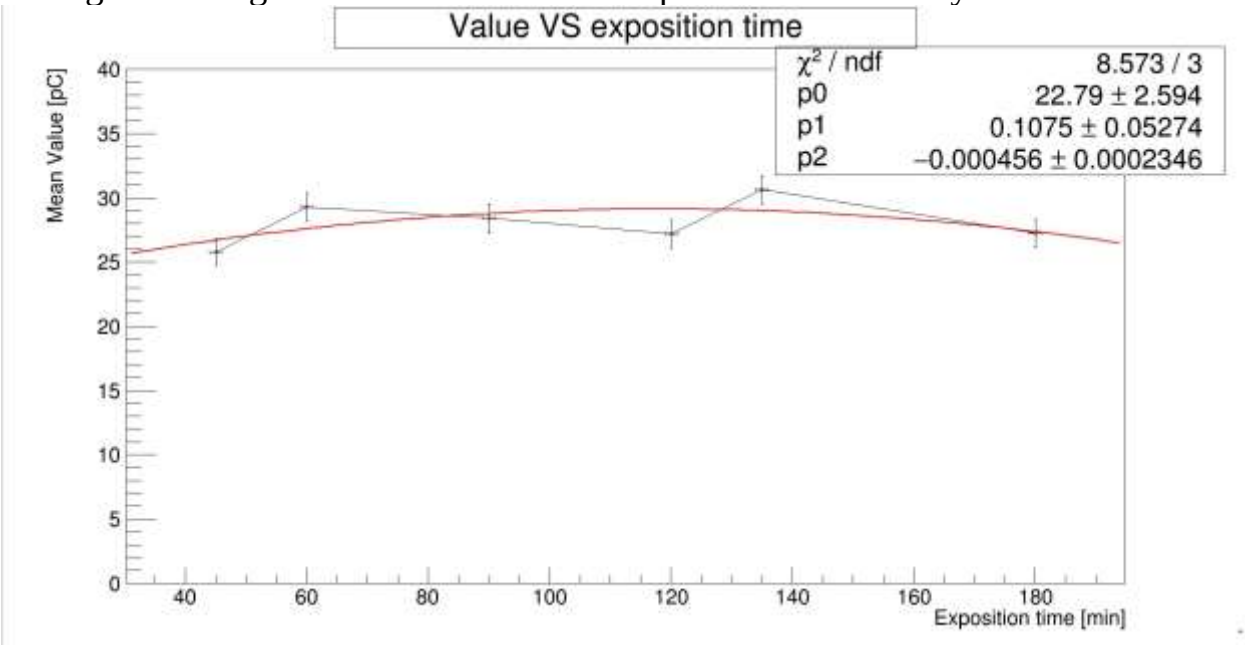

Fig. 9.b Charge value as a function of exposure time fitted with parabolic function

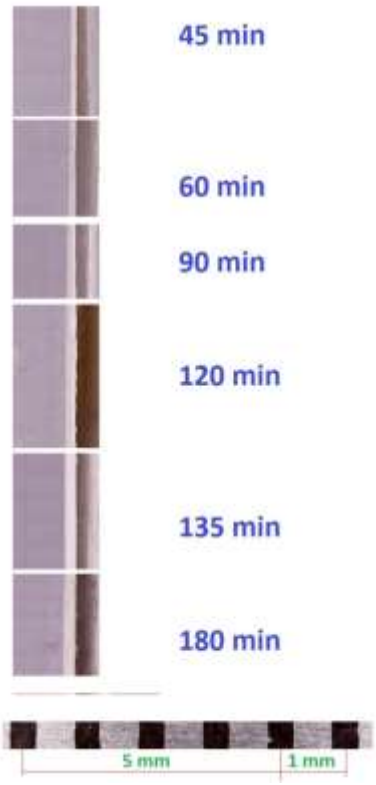

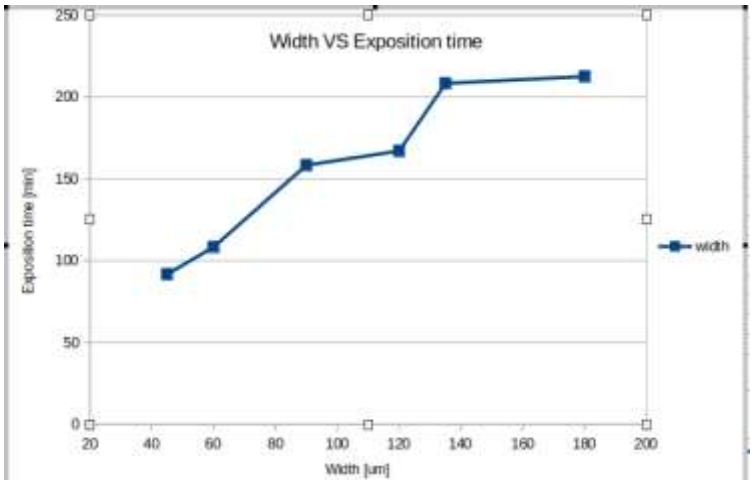

Fig. 10a Fig. 10b

Fig. 10a Transverse pictures of the surface of strips

Fig. 10b Dependence of etching exposition time on cover width

Figure 10a shows strips cross-section pictured by the 25x- zoom camera, so that we could calculate the real thickness of the coating later. By calculating the thickness using obtained photos, I built a graph of the dependence for the cover thickness on etching time, which shows an increase in thickness over time, although would be at a time greater than 120. Therefore, graphs are also constructed depending on the charge value versus width (Fig. 11a and 11b).

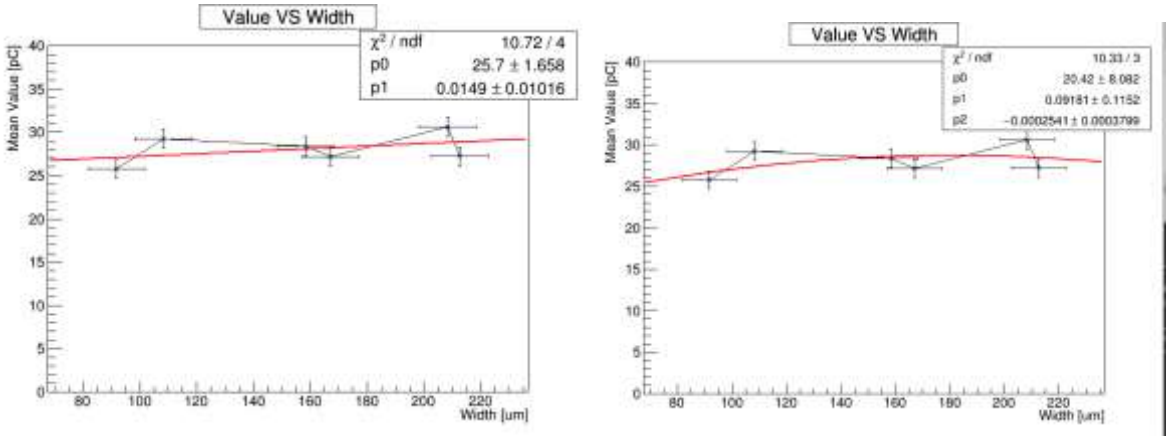

Fig. 11 a,b Charge value as a function of Width

2.3 Transparency registration

These strips were also tested for the transparency and for the reflection using a spectrophotometer (Figure 12), the SolidSpec-3700DUV. The principal scheme is presented in Fig. 13. The wavelength range was measured from 200 to 800 nanometers. The spectrophotometer is equipped with two light sources: an infrared source (a halogen lamp up to 2600 nm) and a deuterium lamp (from 240 nm). The histogram of transparency and the graphs depicting the relationship between transparency and wavelength are shown in Fig. 14.

Fig. 12 SolidSpec-3700DUV - spectrometer

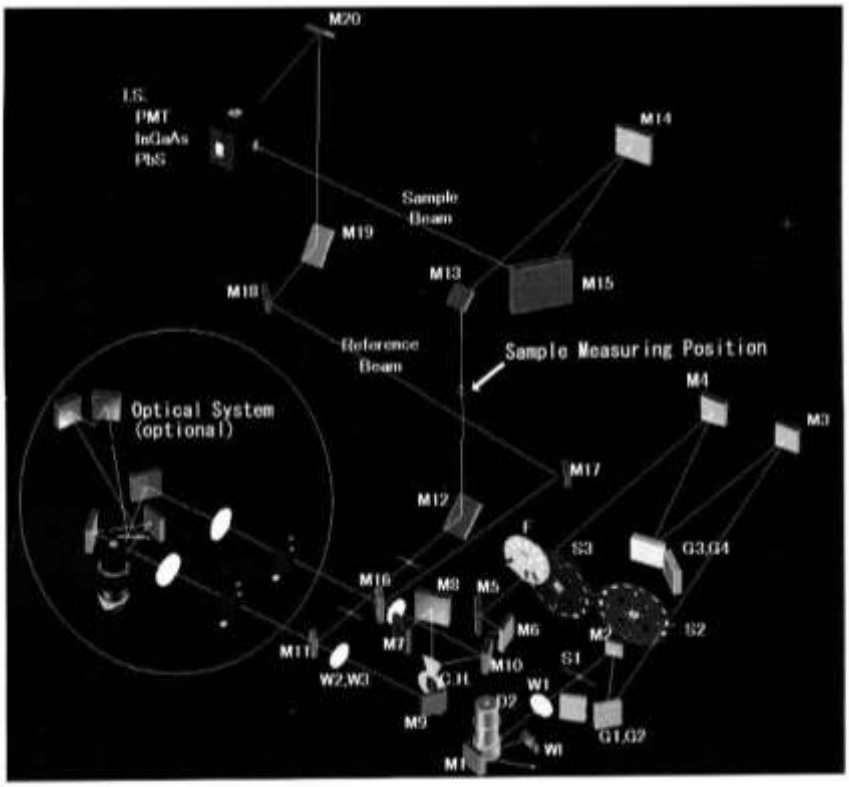

Fig. 13 Optical System: SolidSpec-3700 Series,

D2-Deuterium Lamp
S1-Entrance Slit
S2-Intermediate Slit
S3-Exit Slit
F-Filter
G1,G2-Diffraction Grating (first spectrometer)
G3,G4-Diffraction Grating (second spectrometer)
C.H. - Chopper mirror
I.S. -Integrating Sphere
W1- Halogen Lamp
M1-M20-Mirrors
PbS-PbS Cell
INGaAs-InGaAs Photo-diode
PMT-Photomultiplier Tube
Reference Beam-Beam on Reference Side
Sample Beam-Beam on Sample Side
W1-3-Windows(ϕ30 mm)

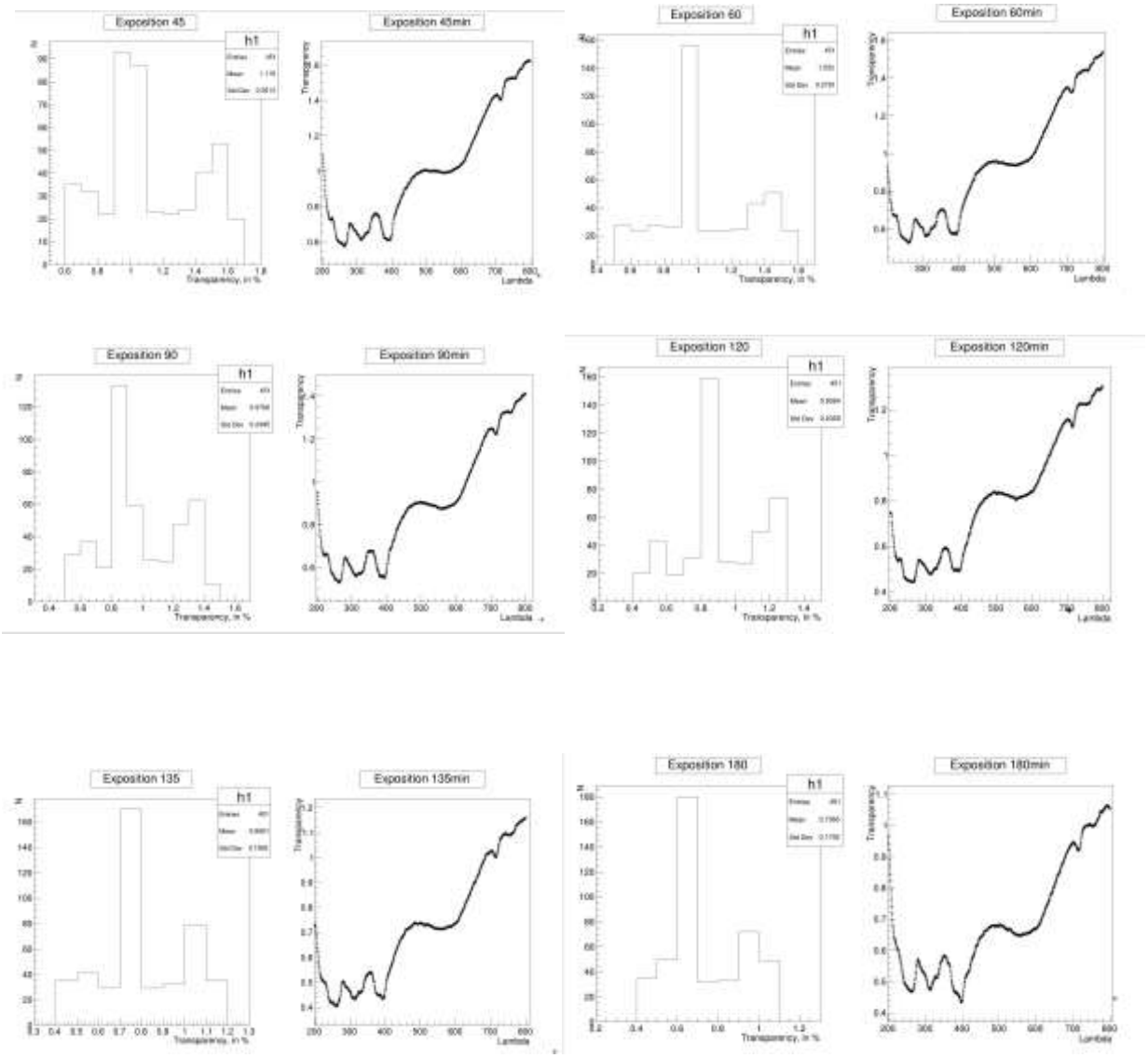

Fig. 14 The histogram of transparency and the graphs depicting the relationship between transparency and wavelength. Note that the light passed the strip cover twice - on entrance to scintillator and on leaving

Figure 15 illustrates the relationship between averaged transparency and exposure time. This dependence is fitted with a linear function, and it is observed that as the exposure time increases, corresponding to the thickness of the scintillator coating, the transparency value decreases consistently.

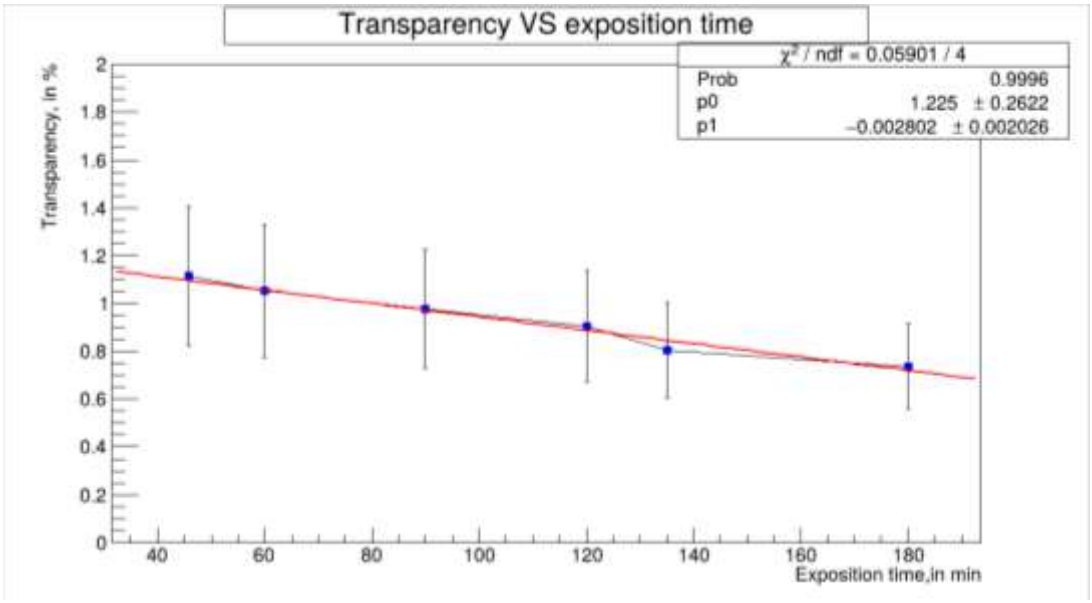

Fig. 15 Dependence of averaged transparency on exposure time

Along with this, I also measured the reflection coefficient of scintillators with different surface etching times. Figure 16 shows the spectrum of light for 200…400 nm, which means that in the UV region. One could note an increase of the light relative to BaSO4 standard caused mainly by scintillating of the strip cover in this region. For the light of 400…800 nm area, the reflection is quite high, almost 70% to BaSO4 standard.

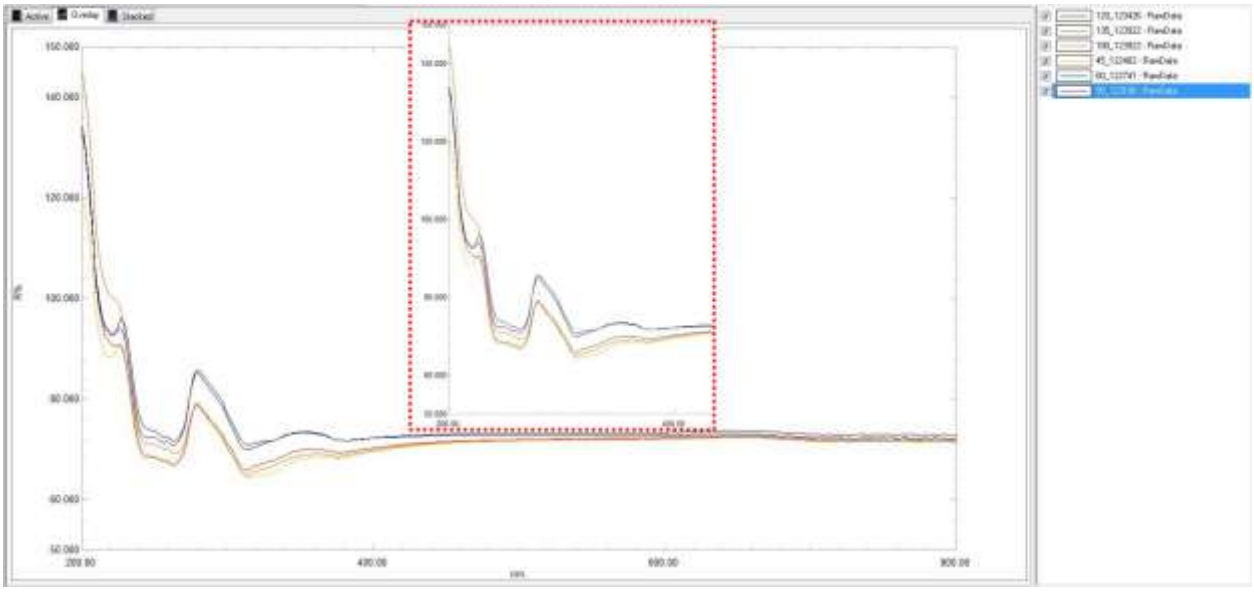

Fig. 16 Diffuse reflection of scintillator strips

III.Research of fluoroplastic membranes

Reflectors are widely used to enhance light yield. Their level of enhancement depends on the reflection coefficient at the emission wavelength of the scintillator. We report UV-Visible reflectance spectra relative to BaSO4 for several common reflectors. Scintillators are widely used in high energy physics (HEP) calorimeters. Also in the MU2E experiment at Fermilab, scintillator wrapping films are used to increase the scintillation light collection efficiency from non-organic crystal (CsI or BaF_2) for the e-calorimeter to detect the charged particle energy (especially for electrons). The light collection efficiency depends on the reflectance of the cover at the scintillator emission wavelength at UV region. At the same time, good light proofing is necessary for the neighbor crystals.

We report the results of a study of relative reflectance spectra of the reflectors: aluminum foil, aluminised mylar film, Tyvek paper. We also studied membranes with different porosity from LLC 'Vladipor', Vladimir.

These membranes have the following structure: the fluoroplastic with different porosity was applied on the substrate-lavsan. We used membranes of the following grades:

UFFK (0.05 μm)
MFFK-1 (0.15 μm)
MFFK-2 (0.25 μm)
MFFK-3 (0.45 μm)
MFFK-4 (0.6 μm)
MFFK-5 (1 μm)

These samples were studied for the transparency, for the diffuse and direct reflection on the same device with which the transparency of scintillators with different exposure times was viewed. BaSO4 was used as a reference for calibration of the spectrometer.

The measurement range was from 200 to 800 nm. The spectra of the membranes were taken from both sides of it: with fluoroplastic on the light way and when substrate-lavsan was first on the light way. Figure 17 shows that the side of the membrane coated with photoplastics reflects well in the UV range (up to 50 percent massively), while the widely used Tyvek paper is only about 40. Also, the substrate-lavsan side of the membrane did not reflect the UV in contrast to Tyvek.

With diffuse reflection, fluoroplastic membranes reflect even more than with direct reflection(Figure 18). The samples were also tested for transparency on the same device (Figure 19).

So, the membranes showed two properties at the same time: very high reflection efficiency for the UV region for the fluoroplastic side on it, and totally blind for UV from the lavsan side and was very low transparency for the same region ensuring good UV light proving of the neighbor crystals.

Since in the experiment scintillators and membranes, which we believe can serve as an alternative to other wrapping materials, should be used in a high radiation level, we need to know the radiation hardness of it. The samples were irradiated by gamma-particles and should be tested again. After that, we can say with more

confidence that these materials have a perspective for wrapping scintillating crystals (CSI or BaF_2) of electromagnetic calorimeters in the MU2E experiment.

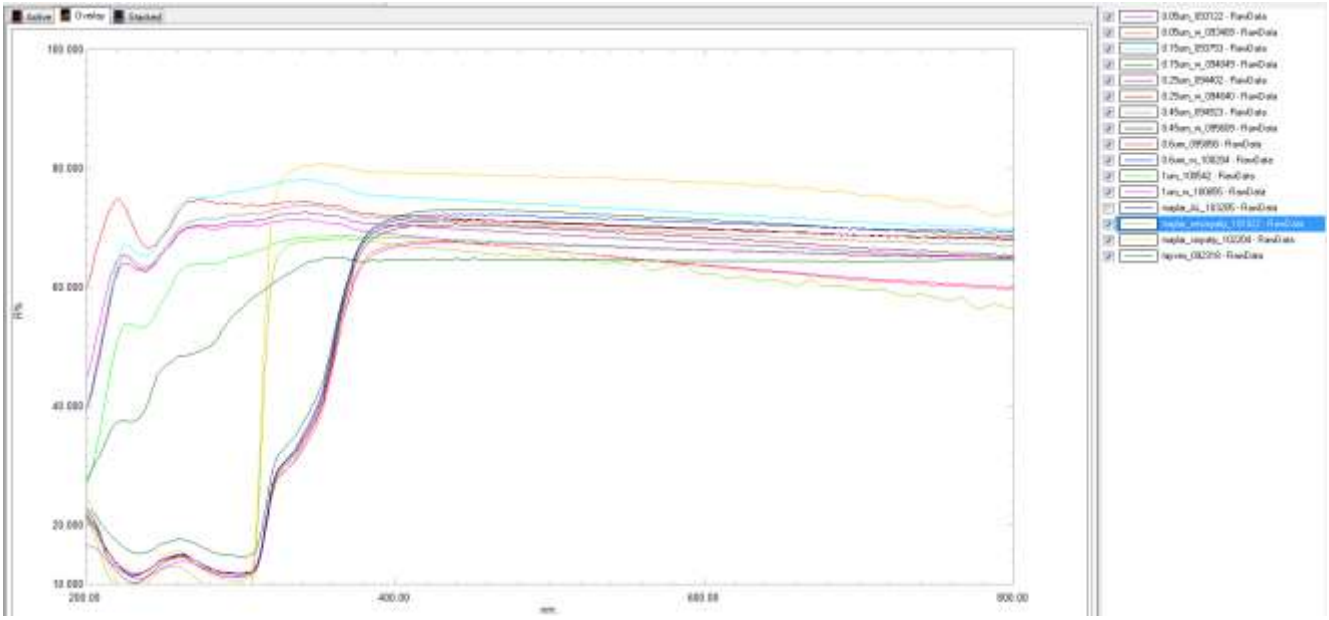

Fig. 17 Direct reflection spectra

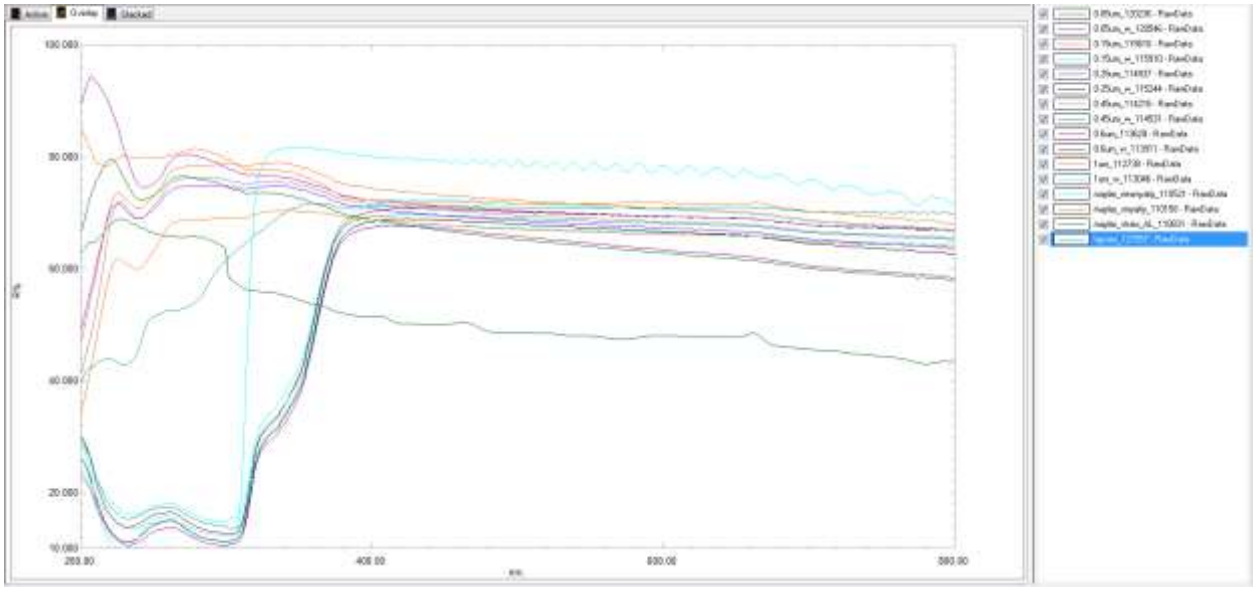

Fig. 17 Diffuse reflection spectra

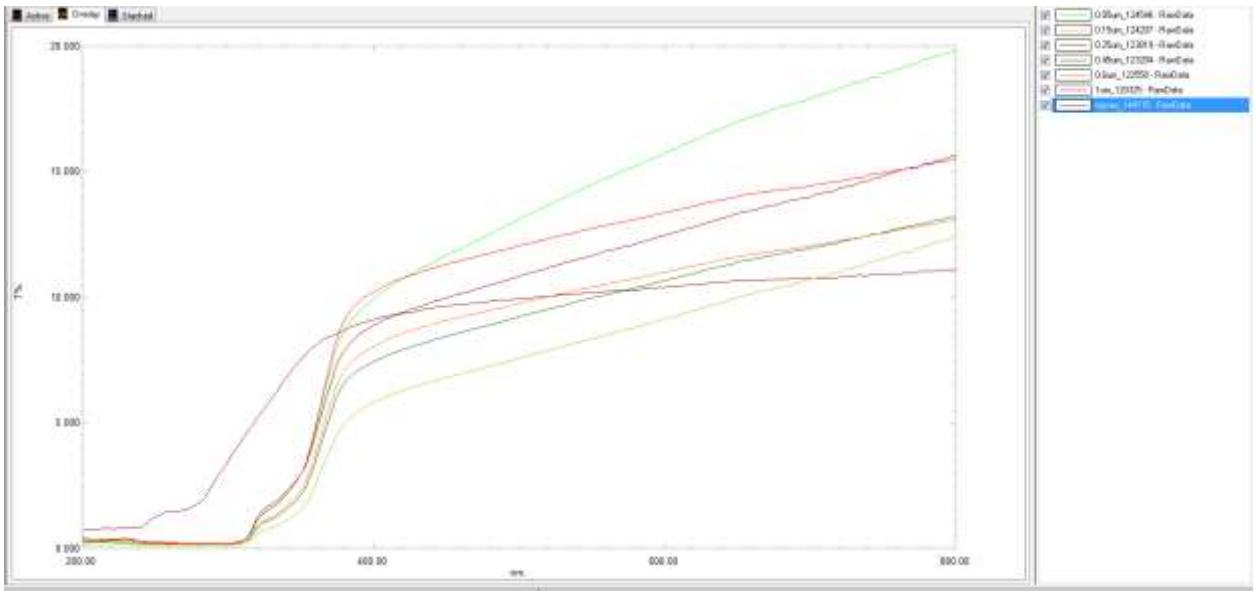

Fig. 17 Transparency spectra

Bibliography

[1] I.Bartoszek,et al., Mu2e Collaboration, Mu2e Technical Design Report, Tech Rep., FERMILAB, 2014, http://dx.doi.org/10.2172/1172555, arXiv:1501.05241.
[2] R. Abramishvili, et al., COMET Collaboration,COMET Phase-I Technical Design Report , Etch. Rep. 3, KEK/J-PARC, 2020, 033C01, http://dx.doi.org/10.1093/ptep/ptz125, arXiv:1812.09018.
[3] https://root.cern.ch/
[4] Fabrication of a Cosmic Ray Veto System for the Mu2e Experiment, arXiv:1910.00690v1 [physics.ins-det] 1 Oct 2019

Acknowledgement

I would like to thank the University Center of JINR for giving me such an incredible opportunity to participate in the Summer Student Program and to broaden my horizon on Networking, Computing and Computational Physics. I am grateful to my supervisors Akram Artikov and Davit Chockheli, who supported my journey throughout the program and gave me an opportunity to not only study such an amazing topic but also make great acquaintances with incredible people. I would like to express my sincere thanks to Ilya Vasilyev,Vladimir Baranov,Aleksandr Boikov and the whole laboratory team for their help and support, who were always ready to answer my questions with that guide I managed to overcome the obstacles presented during my work on START.Special thanks to Elena Karpova for helping resolve any arising problems and answering all my questions.
It is a pleasure to have had the opportunity to work with them and I look forward to counting on their support in the future.